Greenhouse gases emissions from riparian wetlands: An example from the Inner Mongolia grassland region in China

Xinyu Liu[1,2], Xixi Lu[1,3], Ruihong Yu[1,2], Heyang Sun[1], Hao Xue[1], Zhen Qi[1], Zhengxu Cao[1], Zhuangzhuang Zhang[1], Tingxi Liu[4]

[1] Inner Mongolia Key Laboratory of River and Lake Ecology, School of Ecology and Environment, Inner Mongolia University, Hohhot 010021, China;

[2] Key Laboratory of Mongolian Plateau Ecology and Resource Utilization, Ministry of Education, Hohhot 010021, China;

[3] Department of Geography, National University of Singapore, 117570, Singapor;

[4] Inner Mongolia Water Resource Protection and Utilization Key Laboratory, Water Conservancy and Civil Engineering College, Inner Mongolia Agricultural University, Hohhot 010021, China

Corresponding author: Ruihong Yu (rhyu@imu.edu.cn) and Tingxi Liu (txliu@imau.edu.cn)

Abstract: Gradual riparian wetland drying is increasingly sensitive to global warming and contributes to climate change. Riparian wetlands play a significant role in regulating carbon and nitrogen cycles. In this study, we analyzed the emissions of carbon dioxide (CO_2), methane (CH_4), and nitrous oxide (N_2O) from riparian wetlands in the Xilin River Basin to understand the role of these ecosystems in greenhouse gas (GHG) emissions. Moreover, the impact of the catchment hydrology and soil property variations on GHG emissions over time and space were evaluated. Our results demonstrate that riparian wetlands emit larger amounts of CO_2 (335–2790 $mg \cdot m^{-2} \cdot h^{-1}$ in wet season and 72–387 $mg \cdot m^{-2} \cdot h^{-1}$ in dry season) than CH_4 and N_2O to the atmosphere due to high plant and soil respiration. The results also reveal clear seasonal variations and spatial patterns along the transects and in the longitudinal direction. N_2O emissions showed a spatiotemporal pattern similar to that of CO_2 emissions. Near-stream sites were the only sources of CH_4 emissions, while the other sites served as sinks for these emissions. Soil moisture content and soil temperature were the essential factors controlling the GHG emissions, and abundant aboveground biomass promoted the CO_2, CH_4, and N_2O emissions. Moreover, compared to different types of grasslands, riparian wetlands were the potential hotspots of GHG emissions in the Inner Mongolian region. Degradation of downstream wetlands has resulted in reducing the soil carbon pool by approximately 60%, reducing CO_2 emissions by approximately 35%, and converting the

wetland from a CH_4 and N_2O source to a sink. Our study showed that anthropogenic activities have extensively changed the hydrological characteristics of the riparian wetlands and might accelerate carbon loss, which could further affect the GHG emissions.

Key words: Riparian wetlands, Grasslands, Greenhouse gas, Spatial-temporal distribution, Impact factor, Xilin River Basin

1. Introduction

With the increasing impacts of global warming, the change in the concentrations of greenhouse gases (GHGs) in the atmosphere is a source of concern in the scientific community (Cao et al., 2005). According to the World Meteorological Organization (WMO, 2018), the concentrations of carbon dioxide (CO_2), methane (CH_4), and nitrous oxide (N_2O) have increased by 146%, 257%, and 122%, respectively, since 1750. Despite their lower atmospheric concentrations, CH_4 and N_2O absorb infrared radiation approximately 28 and 265 times more effectively at centennial timescales than CO_2 (IPCC, 2013). On a global scale, CO_2, CH_4, and N_2O contribute 87% to the GHG effect (Ferrón et al., 2007).

Wetlands are unique ecosystems that serve as transition zones between terrestrial and aquatic ecosystems. They play an important role in the global carbon cycle (Beger et al., 2010; Naiman and Decamps, 1997). Wetlands are sensitive to hydrological changes, particularly in the context of global climate change (Cheng and Huang, 2016). Moreover, wetland hydrology is affected by local anthropogenic activities, such as the construction of reservoirs, resulting in gradual drying. Although wetlands cover only 4–6% of the terrestrial land surface, they contain approximately 12–24% of global terrestrial soil organic carbon (SOC), thus acting as carbon sinks. Moreover, they release CO_2, CH_4, and N_2O into the atmosphere and serve as carbon sources (Lv et al., 2013). In general, the carbon accumulation by plant's photosynthesis is higher than the consumption (plant respiration, animal respiration, and microbial decomposition) in the wetland, thus the net effect of the wetland is acted as a carbon sink. Wetlands are increasingly recognized as an essential part of nature, given their simultaneous functions as carbon sources and sinks. Excessive

rainfall will cause an expansion in wetland areas and a sharp increase in the soil moisture content, thus enhancing respiration, methanogenesis, nitrification, and denitrification rates (Mitsch et al., 2009). On the contrary, reduced precipitation or severe droughts will result in a decrease in water levels, causing the wetlands to dry up. The accumulated carbon will be released back into the atmosphere through oxidation. Due to the increasing impact of climate change and human activity, the drying of wetlands has been widely observed in recent years (Liu et al., 2006); more than half of global wetlands have disappeared since 1900 (Mitsch and Gosselink, 2007), and this tendency is expected to continue in the future. The loss of wetlands may directly shift the soil environment from anoxic to oxic conditions, and modify the CO_2 and CH_4 source and sink functions of wetland ecological systems (Waddington and Roulet, 2000; Zona et al., 2013).

The Xilin River Basin in China is characterized by a marked spatial gradient in soil moisture content. It is a unique natural laboratory that may be used to explore the close relationships between the spatiotemporal variations in hydrology and riparian biogeochemistry. Wetlands around the Xilin River play an irreplaceable role with regard to local climate control, water conservation, the carbon and nitrogen cycles, and husbandry (Gou et al., 2015; Kou, 2018). Moreover, the Xilin River region is subjected to seasonal alterations in precipitation and temperature regimes, and construction of the Xilin River Reservoir has resulted in highly negative consequences, such as the drying of downstream wetlands, affecting riparian hydrology as well as microbial activity in riparian soils. GHG emissions in riparian wetlands vary immensely. Understanding the interactions between GHG emissions and hydrological changes in the Xilin River riparian wetlands has thus become increasingly important. Moreover, it is necessary to estimate the changes in GHG emissions as a result of wetland degradation at local and global scales.

In this work, GHG emissions from riparian wetlands and adjacent hillslope grasslands of the Xilin River Basin were investigated. GHG emissions, soil temperature, and soil moisture content were measured in dry and wet seasons. The main objectives of this study were to (1) investigate the temporal and spatial variations in CO_2, CH_4, and N_2O emissions from the wetlands in the riparian zone, and examine the main factors affecting the GHG emissions, (2) compare the GHG emissions from the riparian wetlands and different types of grasslands, and (3) evaluate the impact of wetland degradation in the study area on GHG emissions.

2. Materials and methods

2.1 Study site

The Xilin River is situated in the southeastern part of the Inner Mongolia Autonomous Region in China (E115°00'–117°30', N43°26'–44°39'). It is a typical inland river of the Inner Mongolia grasslands. The river basin area is 10,542 km^2, the total length is 268.1 km, and the average altitude is 988.5 m. According to the meteorological data provided by the Xilinhot Meteorological Station (Xi et al., 2017; Tong et al., 2004), the long-term annual mean air temperature is 1.7°C, and the maximum and minimum monthly means are 20.8°C in July and −19.8°C in January, respectively. The average annual precipitation was 278.9 mm for the period of 1968–2015. Precipitation is distributed unevenly among the seasons, with 87.41% occurring between May and September.

Soil types in the Xilin River Basin are predominantly chernozems (86.4%), showing a significant zonal distribution as light chestnut soil, dark chestnut soil, and chernozems from the northwest to southeast. Soil types in this basin also present a vertical distribution with elevation. The chernozems are primarily soluble chernozems and carbonate chernozems, distributed at altitudes above 1350 m with a relatively fertile and deep soil layer. Dark chestnut soil, boggy soil, and dark meadow with high humus content are distributed between the altitudes of 1150 and 1350 m. Light chestnut soil, saline meadow soil, and meadow solonchak with low soil humus, a thin soil layer, and coarse soil texture are distributed between the altitudes of 902 and 1150 m (Xi et al., 2017).

2.2 Field measurements and laboratory analyses

In this study, five representative transects were selected as the primary measurement sites in the entire Xilin River. Each transect cuts through the riparian wetlands near the river and hillslope grasslands further away from it (Fig. 1).

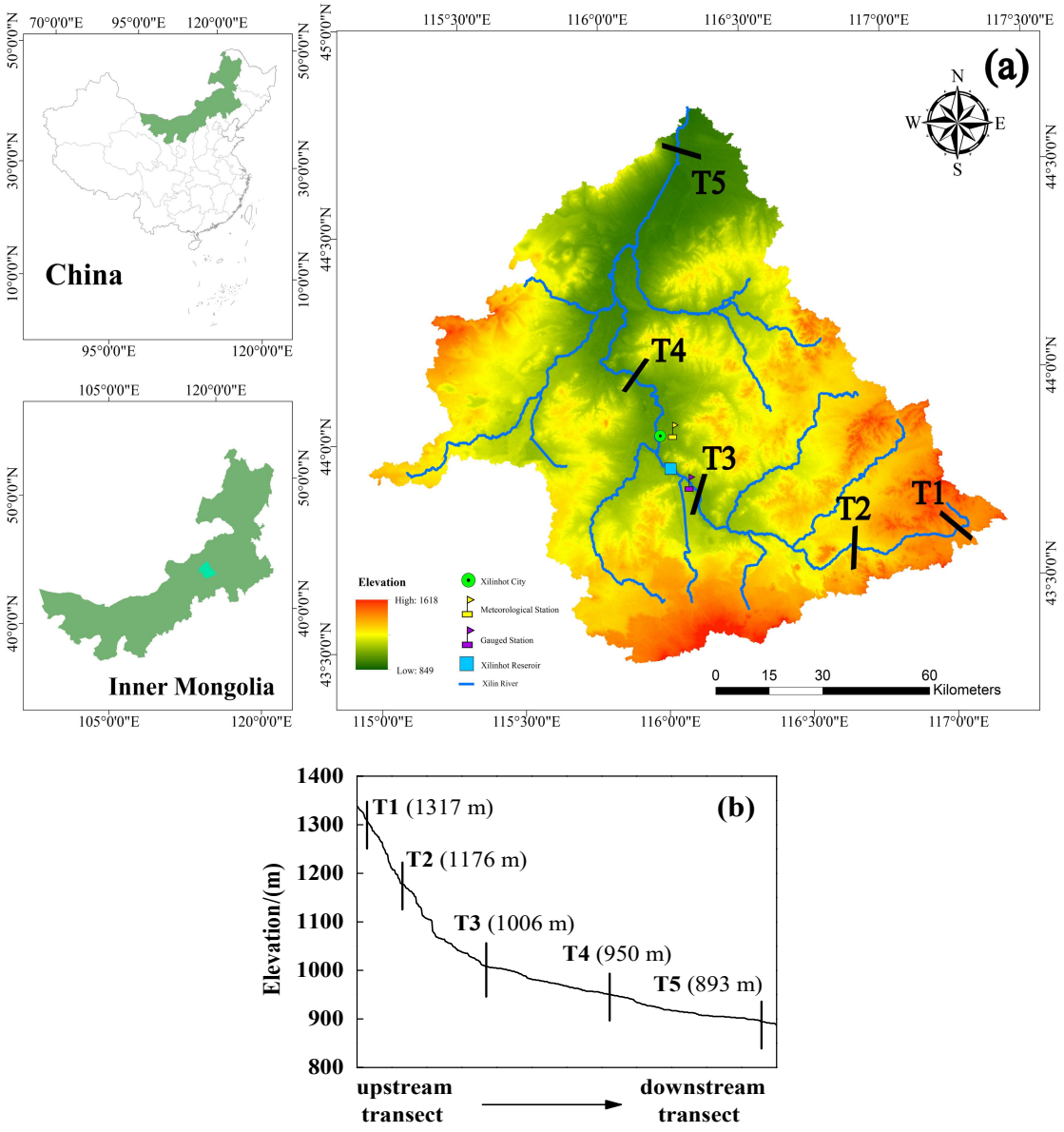

Fig. 1 (a) Location of the Xilin River Basin and distribution of five riparian-hillslope transects (T1–T5). (b) Elevation details of each transect in the Xilin River Basin.

The layout of the sampling points of each transect is shown in Fig. 2. Each sampling point from T1–T5 was extended from the river to both sides, to the grassland on the slopes, using 5–7 sampling points for each transect and resulting in 24 points in total. The sampling sites on the left and right banks were defined as L1–L3 and R1–R4 from the riparian wetlands to the hillslope grasslands. As transect T3 was located on a much wider flood plain, none of its sampling points were located on the hillslope grassland. The last transect (T5) was located downstream in the dry lake and contained seven sampling points. They were defined as S1–S7, where S1, S2, and S7

were located along the lake shore (the lakeside zone), and S3–S6 were located in the dry lake bed (S3 and S4 in the mudbank, S5 in saline–alkali soil, and S6 in sand–gravel geology). Moreover, characterizations for T1, T2, and T3 transects were the continuous river flow and T4 and T5 transects were the intermittent river flow.

The CO_2, CH_4, and N_2O emissions from each site were measured in August (wet season) and October (dry season) in 2018 using a static dark chamber and the gas chromatography method. The static chambers were made of a cube-shaped polyvinyl chloride (PVC) pipe (dimensions: 0.4 m × 0.2 m × 0.2 m). A battery-driven fan was installed horizontally inside the top wall of the chamber to ensure proper air mixing during measurements. To minimize heating from solar radiation, white adiabatic aluminum foil was used to cover the entire aboveground portion of the chamber. During measurements, the chambers were driven into the soil to ensure airtightness and connected with a differential gas analyzer (Li-7000 CO_2/H_2O analyzer, LI-COR, USA) to measure the changes in the soil CO_2 concentration. The air in the chamber was sampled using a 60 mL syringe at 0, 7, 14, 21, and 28 min. The gas samples were stored in a reservoir bag and taken to the laboratory for CH_4 and N_2O measurements using gas chromatography (GC-2030, Japan). The measurements were scheduled for 9:00–11:00 a.m. or 3:00–5:00 p.m.

Soil temperature (ST) was measured at depths of 0–10 cm and 10–20 cm with a geothermometer (DTM-461, Hengshui, China). Plant samples were collected in a static chamber and oven-dried in the laboratory to obtain aboveground biomass (BIO). A 100 cm^3 ring cutter was used to collect surface soil samples at each site, which were placed in aluminum boxes and immediately brought back to the laboratory to measure soil mass moisture content (SMC) and soil bulk density (ρ_b) using national standard methods (NATESC, 2006). Topsoil samples were collected, sealed in plastic bags, and brought back to the laboratory to measure soil pH, electrical conductivity (EC), total soil organic carbon (TOC), and soil C:N ratio.

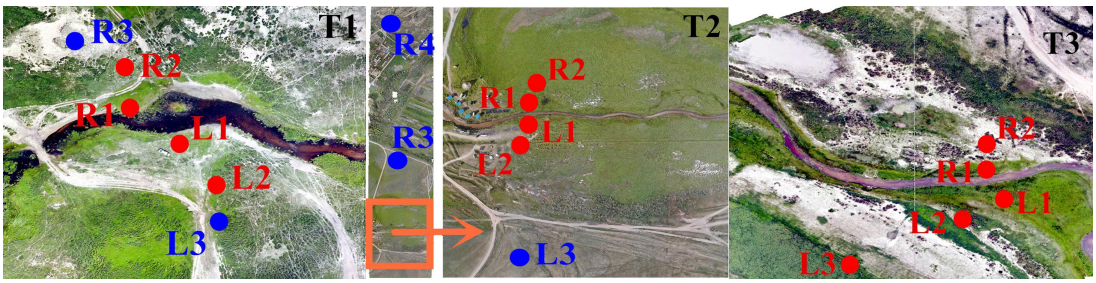

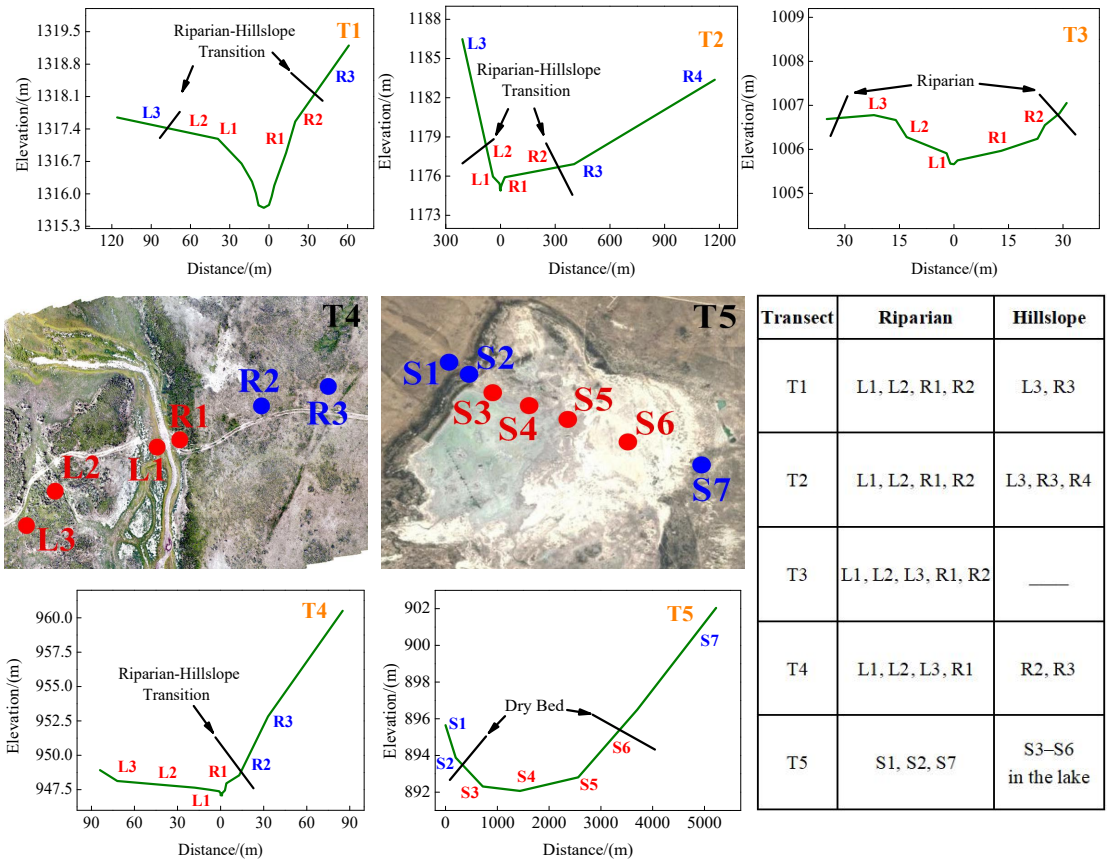

Transect	Riparian	Hillslope
T1	L1, L2, R1, R2	L3, R3
T2	L1, L2, R1, R2	L3, R3, R4
T3	L1, L2, L3, R1, R2	____
T4	L1, L2, L3, R1	R2, R3
T5	S1, S2, S7	S3–S6 in the lake

Fig. 2 Distributions of sampling points in transects T1–T5 (The images are authors' own)

Table 1. Physical and chemical properties (Mean ± SD) of soils at various sites within each transect

Transect	Zone	Samples number	SMC10-V	SMC20-V	Soil C:N	TOC ($g \cdot kg^{-1}$)	BIO (g)	ρ_b	pH	EC (μs/cm)	SSM (%)
T1	Riparian	12	12.16 ± 7.55	12.88 ± 12.05	12.46 ± 0.91	30.16 ± 6.54	14.67 ± 5.44	1.28 ± 0.07	7.25 ± 0.62	154.71 ± 23.70	47.77 ± 7.04
	Hillslope	6	2.72 ± 0.91	5.05 ± 3.09	11.41 ± 0.09	10.77 ± 4.72	6.70 ± 1.48	1.45 ± 0.03	7.22 ± 0.40	82.02 ± 16.37	31.02 ± 1.32
T2	Riparian	12	26.75 ± 19.52	12.19 ± 7.82	11.70 ± 1.14	19.96 ± 5.71	24.76 ± 9.65	1.23 ± 0.05	8.95 ± 0.45	303.88 ± 102.16	51.21 ± 6.49
	Hillslope	9	5.85 ± 4.82	3.03 ± 1.43	9.77 ± 0.88	14.87 ± 11.21	6.10 ± 3.19	1.38 ± 0.13	8.10 ± 0.55	162.97 ± 128.18	35.09 ± 6.75
T3	Riparian	12	28.04 ± 22.95	14.53 ± 8.98	15.80 ± 4.16	22.40 ± 9.69	6.37 ± 2.95	1.35± 0.19	9.50 ± 0.67	1233.20 ± 829.83	47.56 ± 11.65
	L3	3	116.37 ±	113.36 ±	16.8 ±	36.1 ±	107.75	0.592 ±	8.5 ±	403 ± 57.21	>100

			56.91	23.17	0.58	1.84	±16.94	0.02	0.17		
T4	Riparian	12	5.42 ± 3.34	4.07 ± 4.31	12.52 ± 2.06	9.96 ± 1.25	11.97 ± 4.50	1.30 ± 0.08	8.84 ± 0.22	461.72 ± 314.27	44.08 ± 7.07
	Hillslope	6	3.35 ± 2.06	4.27 ± 1.94	9.97 ± 0.50	9.65 ± 1.05	7.84 ± 2.48	1.30 ± 0.09	8.23 ± 0.14	118.5 ± 8.25	39.43 ± 5.55
T5	Dry lake bed	12	17.47 ± 15.08	14.49 ± 13.28	63.74 ± 12.93	31.41 ± 6.55	5.48 ± 2.35	1.16 ± 0.10	9.88 ± 0.18	7320.87 ± 4300.03	58.47 ± 7.16
	Lake shore	9	2.64 ± 1.48	2.82 ± 1.27	15.92 ± 4.71	6.35 ± 1.16	0	1.33 ± 0.09	9.41 ± 0.7	281.82 ± 162.73	37.52 ± 5.34

Note: SMC10-V - soil volumetric moisture content in 0-10 cm; SMC20-V - soil volumetric moisture content in 10-20 cm; Soil C:N - soil carbon-nitrogen ratio; TOC - total soil organic carbon; BIO - aboveground biomass; ρ_b - soil bulk density; pH - soil pH; EC - soil electrical conductivity; SSM - saturated soil moisture.

Table 2. soil particle composition of soils at various sites within each transect

Transect	Zone	soil particle composition		
		Clay % (<0.002 mm)	Silt % (0.02~0.002 mm)	Sand (2.0 ~0.02 mm)
T1	Riparian	2.5	2.7	94.8
	Hillslope	9.6	6.1	85.3
T2	Riparian	5.5	5.8	90.7
	Hillslope	10.8	8.6	80.6
T3	Riparian	4.1	1.1	94.8
T4	Riparian	11.4	1.5	87.1
	Hillslope	12.7	5.9	81.4
T5	Lake shore	5.1	2.1	92.8
	Dry lake bed	46.1	4.8	49.1

2.3 Calculation of GHG emissions

The CO_2, CH_4, and N_2O emissions were calculated using Eq. 1 (Qin et al., 2016):

$$F = \frac{V}{A} \times \frac{\mathrm{d}c}{\mathrm{d}t} \times \rho = H \times \frac{\mathrm{d}c}{\mathrm{d}t} \times \frac{M}{V} \times \left(\frac{273.15}{273.15 + t}\right) \quad (1)$$

Where F denotes the CO_2, CH_4, and N_2O emissions ($mg \cdot m^{-2} \cdot h^{-1}$), H is the height of the static chamber (0.18 m), M is the relative molecular weight (44 for CO_2 and N_2O, and 16 for CH_4), V is the volume of gas in the standard state (22.4 $L \cdot mol^{-1}$), dc/dt is the rate of change of the gas concentration ($10^{-6} \cdot h^{-1}$), and T is the temperature in the black chamber (°C).

The annual cumulative emissions were calculated using Eq. 2 (Whiting G and Chanton J., 2001)

$$M = \sum \frac{F_{i+1} + F_1}{2} \times (t_{i+1} - t_i) \times 24 \quad (2)$$

Where M denotes the total cumulative emissions of CO_2, CH_4, or N_2O ($kg \cdot hm^2$), F is the emission flux of CO_2, CH_4, or N_2O, i is the sampling frequency, t_{i+1}-t_i represents the interval between two adjacent measurement dates.

In this study, a 100-year scale was selected to calculate the global warming potential (GWP) of soil CH_4 and N_2O emissions (Whiting G and Chanton J., 2001):

$$GWP = 1 \times [CO_2] + 25 \times [CH_4] + 298 \times [N_2O] \quad (3)$$

Where 25 and 298 are GWP multiples of CH_4 and N_2O relative to CO_2 on a 100-year time scale, respectively.

2.4 Statistical Analysis

All statistical analyses were performed using SPSS for Windows version 18.0 (SPSS Inc., Chicago, IL, USA). Statistical significance was set at $P < 0.05$. Pearson correlation analysis was conducted to estimate the relationships between GHGs fluxes and environmental variables. A Wilcoxon test was used to determine the difference of GHGs fluxes in two seasons.

3. Results

3.1 Spatiotemporal patterns of SMC for each transect

The temporal and spatial variations in SMC10 in the following order: wet season > dry season and riparian wetlands > hillslope grasslands (Fig. 3a, c, e). Similar variations were observed in SMC20 (Fig. 3b, d, f). The average SMC10 and SMC20 in the continuous river transects in the riparian zones (37.44% in wet season and 19.40% in dry season; 25.96% in wet season and 17.39% in dry season) were higher than those in the hillslope grasslands (9.12% in wet season and 4.15% in dry season; 6.51% in wet season and 5.96% in dry season). During the study period, both SMC10 and SMC20 changed as the distance from the river increased, and the highest value was observed at the near-stream sites (L1 and R1). SMC10 fluctuations were low in the intermittent transect compared to the upstream transects, with a mean value of 11.79% in wet season and 3.72% in dry season in the riparian areas. The mean SMC10 in the hillslopes was

6.58% in wet season and 2.86% in dry season. SMC20 showed similar fluctuation, 7.22% in wet season and 2.98% in dry season in the riparian areas and 7.56% in wet season and 4.4% in dry season in the hillslopes. In transect T5, average SMC10 and SMC20 at the center of the lake (29.00% in wet season and 13.36% in dry season; 29.30% in wet season and 9.69% in dry season) were higher than those along the lake shore (4.90% in wet season and 3.13% in dry season; 3.34% in wet season and 5.22% in dry season).

Wet season

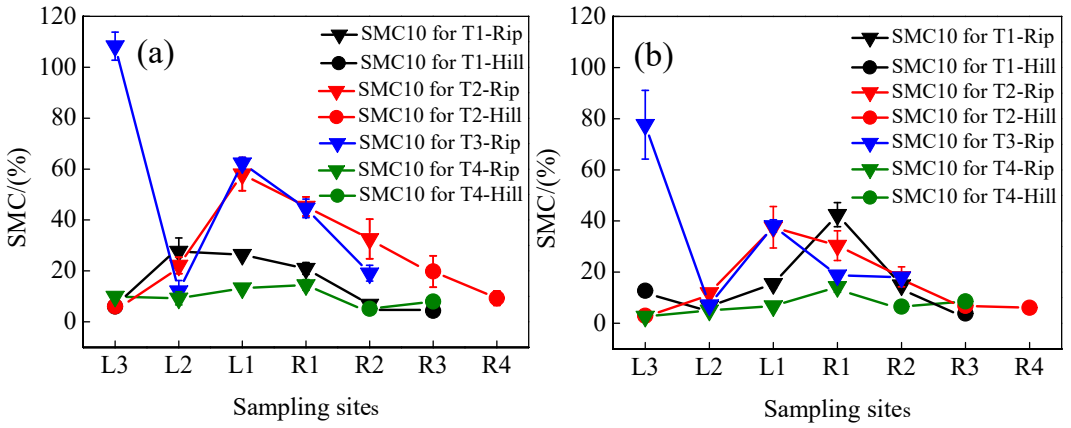

Dry season

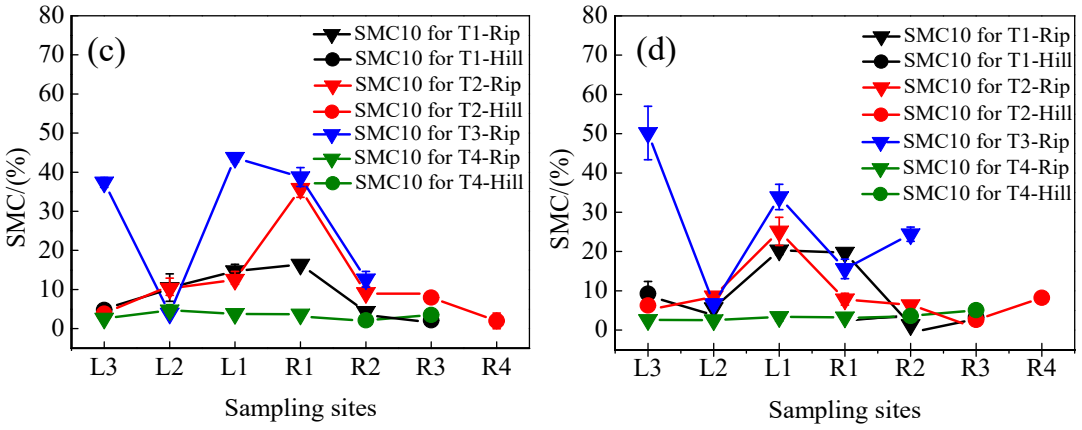

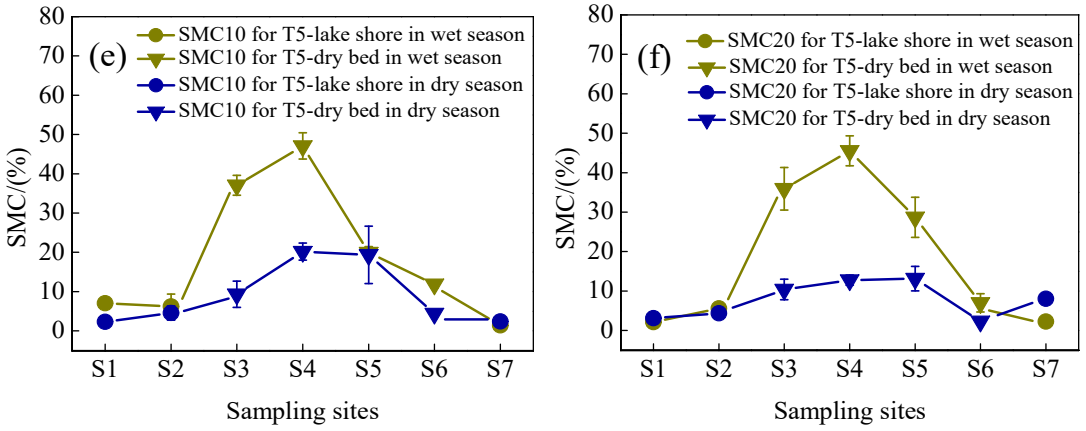

Fig. 3 Soil mass moisture contents (SMCs) at soil depths of 0–10 cm (SMC10) and 10–20 cm (SMC20) for transects T1–T5 in wet season and dry season. Error bars represent the SD about the mean.

3.2 Spatiotemporal patterns of ST in each transect

Spatiotemporal differences in ST during the entire observation period are displayed in Fig. 4. ST variations in wet season (mean value: 27.4°C) were noticeably higher than those in dry season (mean value: 8.97°C). Moreover, ST for riparian sites (mean values: 26.0°C in wet season and 8.41°C in dry season) was slightly lower than that for the hillslope grasslands (mean values: 30.9°C in wet season and 10.3°C in dry season) for the 0–10 cm soil depth, with the exception of transect T5. Similar results were observed for the 10–20 cm soil depth.

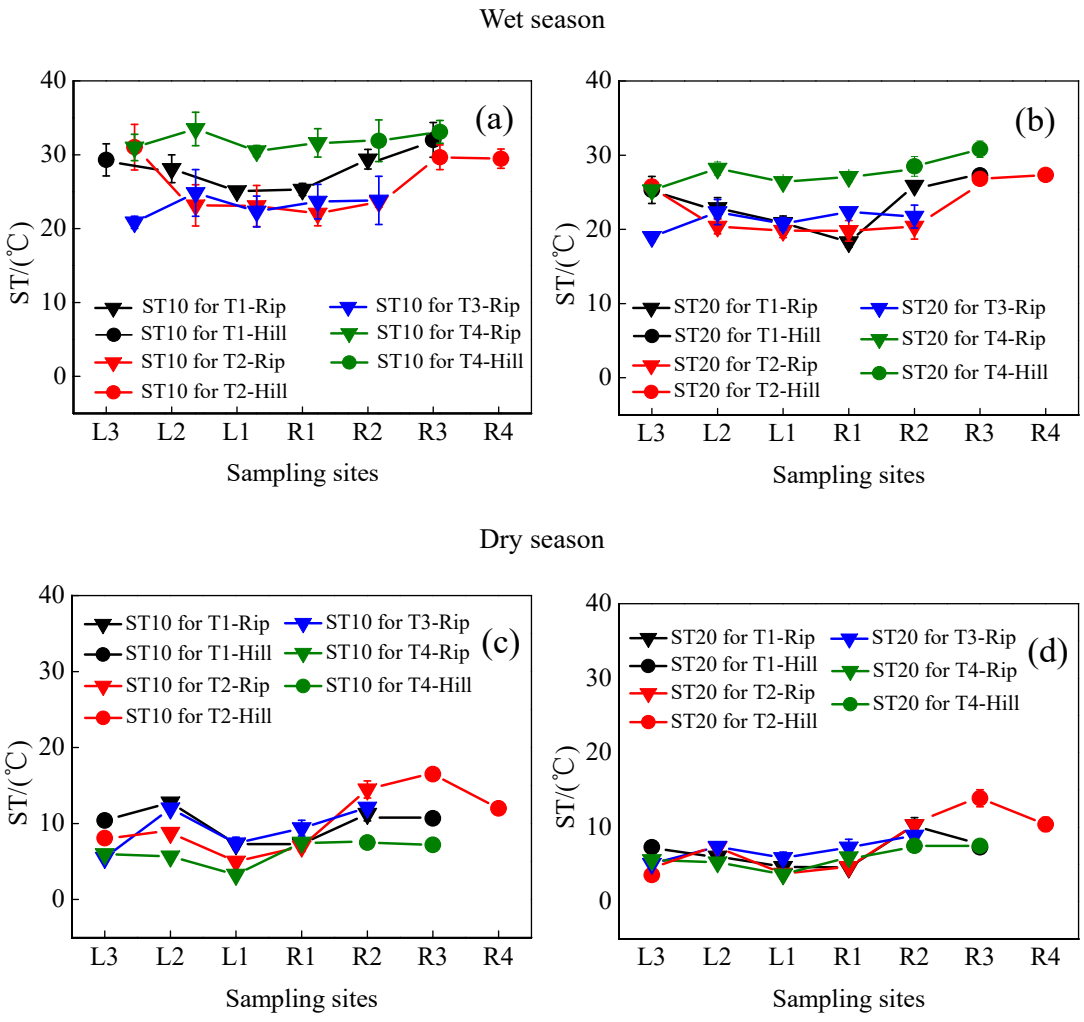

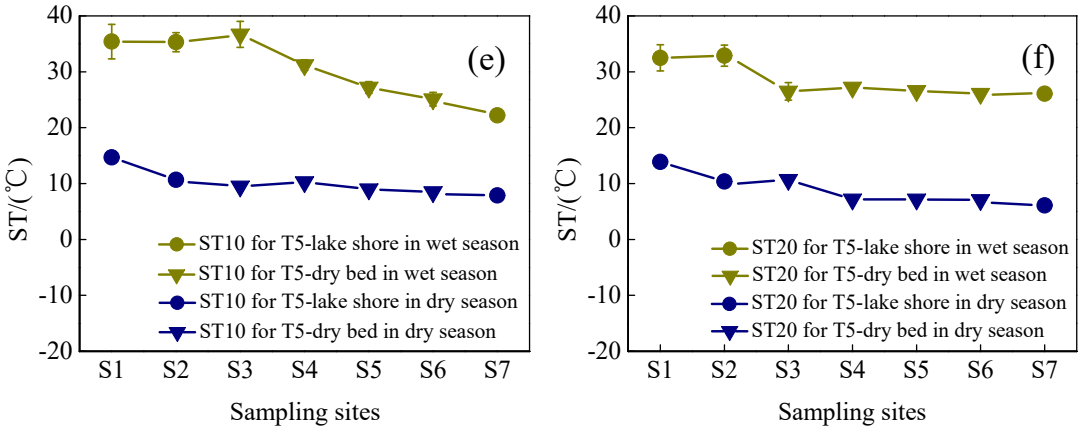

Fig. 4 Soil temperatures (STs) at soil depths of 0–10 cm (ST10) and 10–20 cm (ST20) for transects T1–T5 in wet season and dry season. Error bars represent the SD about the mean.

3.3 Spatiotemporal patterns of GHG emissions in each transect

Figure 5 shows the spatiotemporal variations in GHG emissions in wet season and dry season in each transect. CO_2 emissions in each transect were higher in wet season than in dry season. The average emissions for the riparian wetlands of transects T1–T4 (1582.09 ± 679.34 $mg \cdot m^{-2} \cdot h^{-1}$ in wet season and 163.24 ± 84.98 $mg \cdot m^{-2} \cdot h^{-1}$ in dry season) were higher than those for the hillslope grasslands (1071.54 ± 225.39 $mg \cdot m^{-2} \cdot h^{-1}$ in wet season and 77.68 ± 25.32 $mg \cdot m^{-2} \cdot h^{-1}$ in dry season). Higher CO_2 fluxes occurred in the riparian zones, while lower CO_2 fluxes were observed in the hillslope grasslands in continuous river transects (T1, T2, and T3). Transect T4 exhibited lower CO_2 emissions in the riparian wetlands near the channel than at sites away from the channel. CO_2 emissions in transect T5 in wet season and dry season decreased from the lake shore to the lake center.

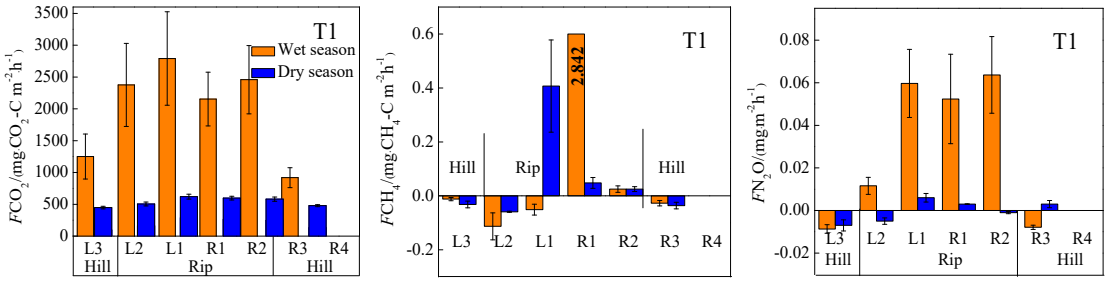

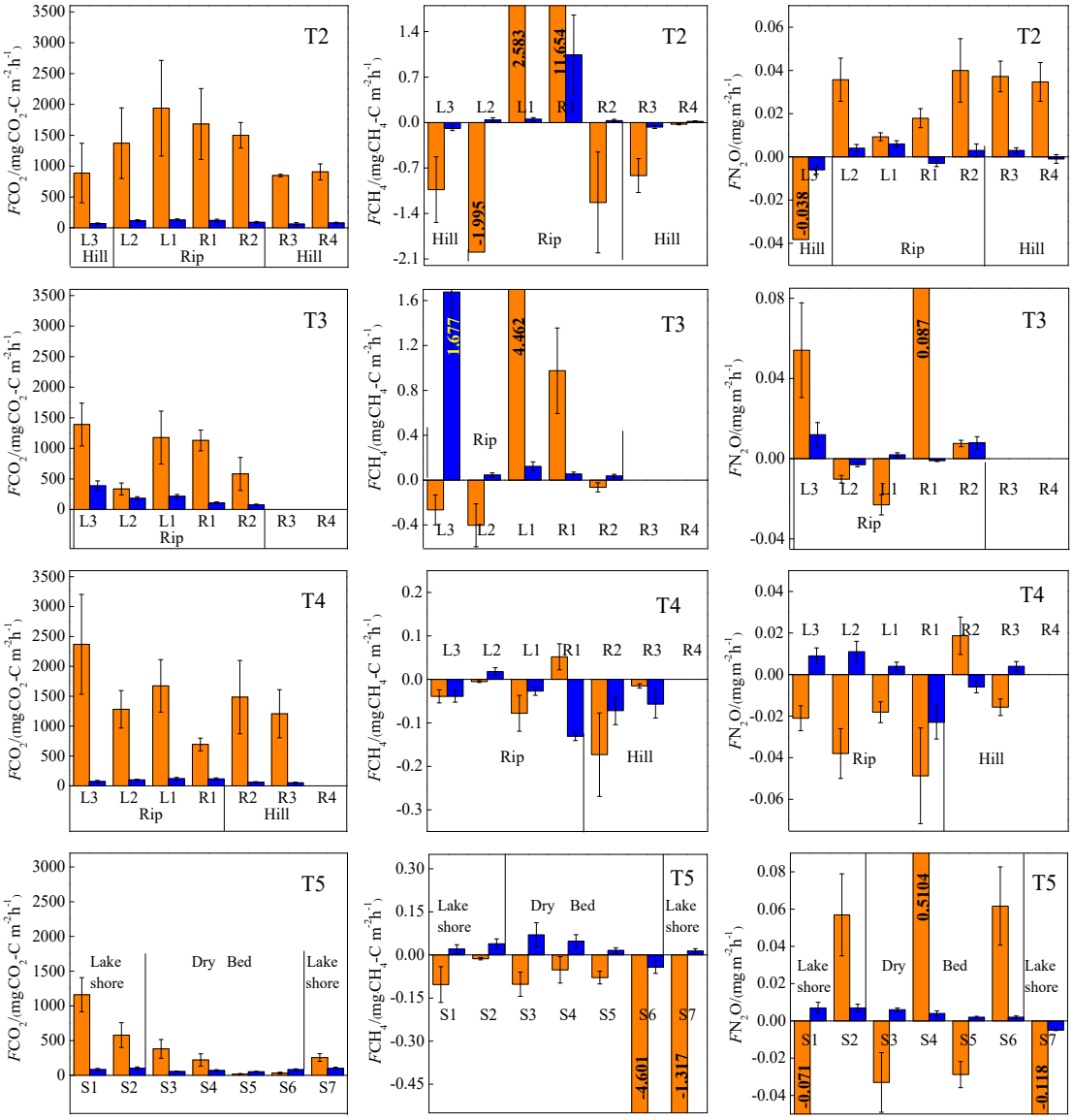

Fig. 5 Spatiotemporal patterns of CO_2 (first column), CH_4 (second column), and N_2O (third column) emissions (F) for each transect. Data are shown for wet season (orange) and dry season (blue) and error bars are the standard deviations.

CH_4 emissions at the transects with continuous river flow (T1, T2, and T3) varied between wet season and dry season, except for T4 (characterized by intermittent river flow) and T5 (the dry lake). In wet season, the near-stream sites (L1 and R1) in T1, T2, and T3 were characterized as high CH_4 sources (average: 3.74 ± 3.81 $mg \cdot m^{-2} \cdot h^{-1}$), but the sites located away from the river gradually turned into CH_4 sinks. Moreover, all the sites in transects T4 and T5 were sinks. CH_4 emissions (mean value: 0.2 ± 0.45 $mg \cdot m^{-2} \cdot h^{-1}$) at the wetland sites were always lower in dry season than those in wet season. However, the sites on the hillslope grasslands served as CH_4

sinks (mean value: −0.05 ± 0.03 mg·m^{-2}·h^{-1}). In transect T5, CH_4 emissions revealed the opposite trend; a CH_4 sink was observed in wet season, but it was transformed into a CH_4 source in dry season.

Similar to the CO_2 and CH_4 emissions, N_2O emissions showed a distinct spatiotemporal pattern for all the transects. N_2O emissions in wet season were higher than those in dry season. These emissions were higher in riparian wetlands than in hillslope grasslands. Moreover, almost all the sites with continuous river flow were N_2O sources, while more than half of the sites with intermittent river flow were sinks.

Table 3 shows that CO_2 fluxes were significantly correlated between the wet season and dry season, while CH_4 and N_2O fluxes were not correlated in two seasons.

Table 3 Significant correlations between GHGs fluxes and two seasons (n-31)

GHG flux	FCO_2 in wet season-FCO_2 in dry season	FCH_4 in wet season-FCH_4 in dry season	FN_2O in wet season- FN_2O in dry season
significant correlations (P)	0.000	0.133	0.290

Note: P<0.05 denote significant correlations and P > 0.05 denote no significant correlations

3.4 Spatiotemporal patterns of GHG emissions in upstream and downstream areas

Figure 6 shows the detailed spatial and seasonal distribution of GHG emissions in wet season and dry season in the longitudinal direction from the upstream (T1, T2, and T3) to the downstream areas (T4 and T5). The CO_2, CH_4, and N_2O emissions were calculated from the average values of the respective emissions in the wetlands and hillslope grasslands in each transect.

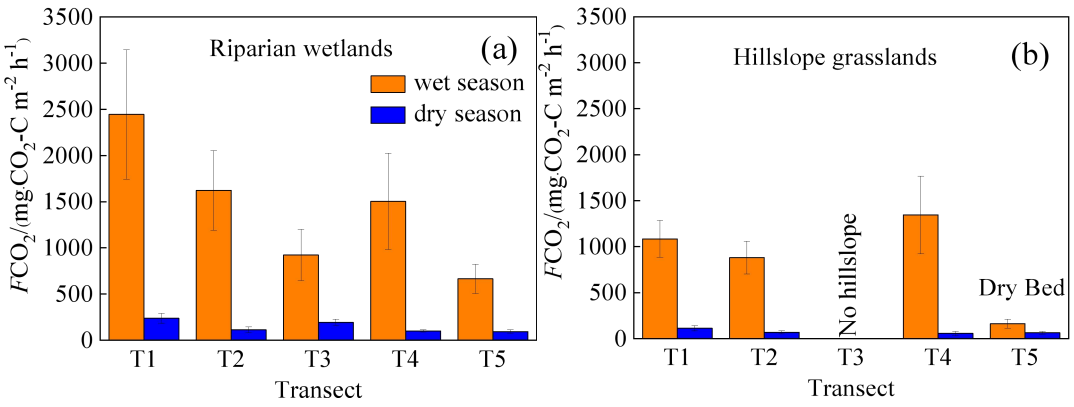

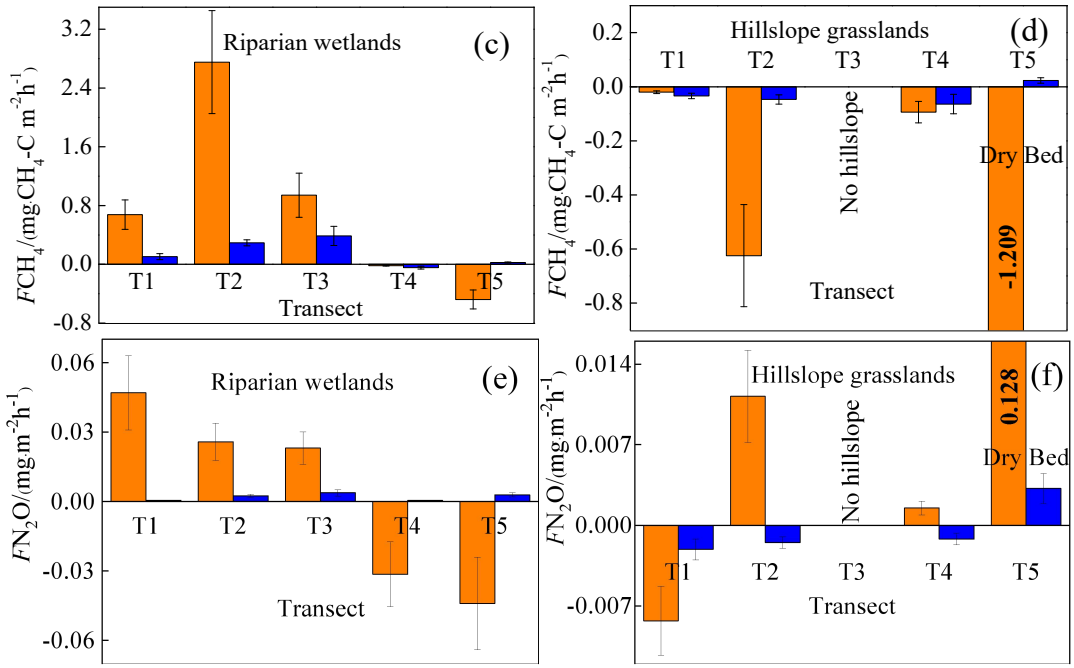

Fig. 6 Spatiotemporal patterns of CO_2 (first line), CH_4 (second line), and N_2O (third line) emissions (F) in the upstream (T1, T2, and T3) and downstream areas (T4 and T5). Bars are the mean values for each transect and error bars are the standard errors.

CO_2 emissions in riparian wetlands (Fig. 6(a)) in wet season decreased from 2444.69 ± 228.58 $mg \cdot m^{-2} \cdot h^{-1}$ in the upstream area to 665.08 ± 347.57 $mg \cdot m^{-2} \cdot h^{-1}$ downstream, and the corresponding values for dry season were 238.12 ± 48.20 $mg \cdot m^{-2} \cdot h^{-1}$ and 94.14 ± 7.67 $mg \cdot m^{-2} \cdot h^{-1}$. However, in hillslope grasslands (Fig. 6(b)), CO_2 emissions exhibited no significant seasonality between upstream and downstream areas, with the mean values of 1103.40 ± 190.44 $mg \cdot m^{-2} \cdot h^{-1}$ in wet season and 79.18 ± 24.52 $mg \cdot m^{-2} \cdot h^{-1}$ in dry season. In addition, CO_2 emissions in transect T5 were lower for both months, with the averages of 162.83 ± 149.15 $mg \cdot m^{-2} \cdot h^{-1}$ and 63.26 ± 12.40 $mg \cdot m^{-2} \cdot h^{-1}$ in wet season and dry season, respectively. The upstream riparian zones exhibited higher CO_2 emissions (894.32 ± 868.47 $mg \cdot m^{-2} \cdot h^{-1}$) than their downstream counterparts (621.14 ± 704.10 $mg \cdot m^{-2} \cdot h^{-1}$). However, mean CO_2 emissions showed no significant differences in grasslands, averaging 524.16 ± 450.10 $mg \cdot m^{-2} \cdot h^{-1}$ upstream and 508.06 ± 534.77 $mg \cdot m^{-2} \cdot h^{-1}$ downstream.

CH_4 emissions showed a marked spatial pattern in the riparian zones from upstream to downstream (Fig. 6(c)). The transects with continuous river flow were CH_4 sources in wet season and dry season, with the average emissions of 1.42 ± 3.41 $mg \cdot m^{-2} \cdot h^{-1}$ and 0.27 ± 0.49 $mg \cdot m^{-2} \cdot h^{-1}$,

304 respectively, while those with intermittent river flow served as CH_4 sinks, with the corresponding
305 mean values of −0.21 ± 0.45 mg·m^{-2}·h^{-1} and −0.02 ± 0.05 mg·m^{-2}·h^{-1}. Moreover, the hillslope
306 grassland sites in all transects were CH_4 sinks (Fig. 6(d)).

307 N_2O emissions in riparian wetlands (Fig. 7(e)) showed spatial patterns similar to those of
308 CH_4 emissions. In wet season, the transects with continuous river flow served as N_2O sources,
309 with the mean value of 0.031 ± 0.031 mg·m^{-2}·h^{-1}, while those with intermittent river flow were
310 N_2O sinks with an average value of −0.037 ± 0.05 mg·m^{-2}·h^{-1}. In dry season, N_2O emissions
311 occurred as weak sources in the longitudinal transects, averaging 0.002 ± 0.007 mg·m^{-2}·h^{-1}.
312 However, N_2O emissions in hillslope grasslands did not show any spatial pattern (Fig. 7(f)).

313 # 4. Discussion

314 ## 4.1 Main factors influencing GHG emissions

315 ### 4.1.1 Effects of SMC on GHG emissions

316 SMC constituted one of the main factors affecting GHG emissions in wetlands. In this study,
317 transects T1–T4 were characterized by a marked spatial SMC gradient (i.e., a gradual decrease
318 include SMC10 and SMC20 from the riparian wetlands to the hillslope grasslands and from
319 upstream to downstream (Fig. 3)). The CO_2, CH_4, and N_2O emissions showed a similar trend. In
320 Table 4, SMC10 is positive correlated with CO_2 emissions ($P < 0.05$), SMC10 and SMC20 are
321 significantly positive correlated with CH_4 emissions ($P < 0.01$), and SMC10 and SMC20 are
322 highly positive correlated with N_2O emissions ($P < 0.05$ and $P < 0.01$, respectively). These results
323 indicated the influence of wetland SMC on GHG emissions.

324 Typically, the optimal SMC values associated with CO_2 emissions in riparian wetlands range
325 from 40 to 60% (Sjögersten et al., 2006), creating better soil aeration and improving soil
326 microorganisms' activity and the respiration of plant roots, thereby promoting CO_2 emissions,
327 whereas excessive SMC reduces soil gas transfer due to the formation of an anaerobic
328 environment in the soil, and microbial activity is lower, favoring the accumulation of organic
329 matter (Hui., 2014). On the contrary, the SMC of hillslope grasslands is less than 10%. Low soil
330 moisture inhibits the growth of vegetation with few vegetation residues and litters. Meanwhile,
331 low soil moisture is not conducive to the survival of soil microorganisms, leading to a decrease in
332 CO_2 emissions than to those in riparian zones (Moldrup et al., 2000; Hui., 2014). Similar results
333 were obtained in our study. The changes in CO_2 emissions in transect T5 were contrary to the

334 change in the SMC10 and SMC20 likely because the optimal range of soil C:N is between 10-12
335 (Pierzynski et al., 1994), but the value in the dry lake bed of T5 is higher than 60, high soil C:N
336 resulted in nitrogen limitation in the process of decomposition of organic matter by
337 microorganisms. Furtherly, other sediment properties (like Soil pH>9.5) for this transect were not
338 conducive to the survival of microorganisms (Table 1), and the increase in SMC did not increase
339 the respiration activity of microorganisms.

340 The largest CH_4 emissions were observed at the near-stream sites (i.e., L1 and R1) in T1, T2,
341 and T3, with the average SMC of 30.29%, while the SMC values at the other sites, which were
342 either weak sources or sinks, averaged at 14.57%. These results indicate that a higher SMC is
343 favorable for CH_4 emissions because a higher SMC denotes a soil in a reduced state, which is
344 beneficial for CH_4 production and inhibits CH_4 oxidation. A similar result was reported by Xu et al.
345 (2008). They conducted experiments of CH_4 emissions from a variety of paddy soils in China, and
346 showed that CH_4 production rates increased with the increase in SMC at the same incubation
347 temperature. Meng et al. (2001) also reported that water depth was the main factor affecting CH_4
348 emissions from wetlands. When the water level dropped below the soil surface, the decomposition
349 of organic matter accelerated, and CH_4 emissions decreased. If the oxide layer is large, the soil is
350 transformed into a CH_4 sink (Meng net al., 2011).

351 The N_2O fluxes showed a clear spatial pattern associated with the changes in SMC. The
352 moisture content of wetland soils directly affects the aeration status of the soil. Besides, the
353 aeration status affects the partial pressure of oxygen, which has an important impact on
354 nitrifying/denitrifying bacteria's activity and ultimately affects soil N_2O emissions (Zhang et al.,
355 2005). Table 4 shows that N_2O emissions are significantly positively correlated with SMC10 and
356 SMC20 ($P < 0.01$). Generally, when SMC was below the saturated water content, the
357 microorganisms were in an aerobic environment, and N_2O mainly came from the nitrification
358 reaction. N_2O emissions increases with the increase of SMC (Niu et al., 2017; Yu et al., 2006). In
359 our study, the sampling sites with higher SMC (riparian zones and some hillslope grassland zones
360 in the upstream transects) have higher N_2O emissions. When SMC increases to the saturated water
361 content or is in a flooded state, the system was an anaerobic environment, and the Nos activity
362 was higher due to excessively high SMC, which was conducive to denitrification and eventually
363 produced N_2 (Niu et al., 2017; Yu et al., 2006), such as site L1 in transect T3 in this study. Ulrike

et al. (2004) showed that denitrification was the main process under flooded soil conditions in wetland soils, and the release of N_2 exceeds N_2O. These findings are consistent with those of Liu et al. (2003), who showed that SMC is an essential factor affecting N_2O emissions.

Nitrification:

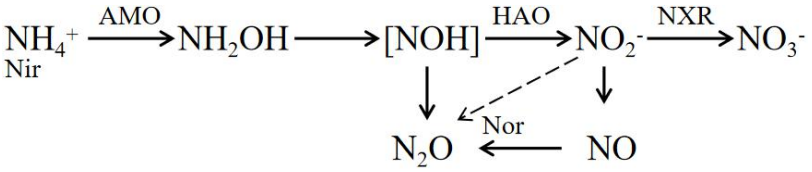

Denitrification:

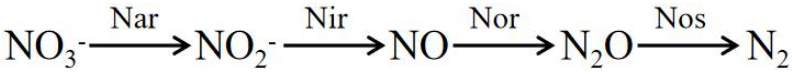

The enzymes involved in the formula include Ammonia monooxygenase (AMO), Hydroxylamine oxidase (HAO), Nitrite REDOX enzyme (HAO), nitrate reductase (Nar), nitrite reductase (Nir), Nitric oxide reductase (Nor) and Nitrous oxide reductase (Nos).

4.1.2 Effects of ST on GHG emissions

ST was another important factor affecting the CO_2 emissions in this study, as this parameter was significantly correlated with CO_2 emissions ($P < 0.01$) (Table 4). The activity of soil microorganisms increases with rising soil temperatures, leading to increased respiration, and consequently higher CO_2 emissions (Heilman et al., 1999). Previous studies reported that ST partially controls seasonal CO_2 emission patterns (Inubushi et al., 2003). Therefore, CO_2 emissions in wet season were significantly higher than those in dry season in this study.

CH_4 emissions showed a clear seasonal pattern because high summer temperatures improve the activity of both CH_4-producing and -oxidizing bacteria (Ding et al., 2010). However, Table 4 indicates that the correlation between CH_4 emissions and temperature is not significant because SMC could be more critical than temperature in our study region with very dry climate. SMC showed a positive correlation with GHG emissions. In addition, SMC affected ST to a certain extent, while the interactions between SMC and ST had a mutual influence on CH_4 emissions. During the study period, the near-stream sites (L1 and R1) maintained a super-wet state on the ground surface for a long time, which was beneficial for the production of CH_4. However, the wetlands maintained a state without water accumulation on the soil surface in August, which was conducive to the oxidative absorption of CH_4. SMC thus masked the effect of ST on CH_4

emissions.

Previous studies indicated that temperature is an important factor affecting N_2O emissions (Sun et al., 2011) through primary mechanisms impacting the nitrifying and denitrifying bacteria in the soil. Table 4 shows that the correlations between N_2O emissions and ST10 and ST20 are poor ($P > 0.05$). This can be attributed to the wide suitable temperature range for nitrification-denitrification and weak sensitivity to temperature. Malhi et al. (1982) found that the optimum temperature for nitrification was 20 ℃, and it will inhibit entirely at 30 ℃. However, Brady (1999) believed that the suitable temperature range for nitrification was 25～35℃, and the nitrification inhibits below 5 ℃ or above 50 ℃. It showed that the temperature requirements of nitrifying microorganisms in wetland soils were different in different temperature belts. The suitable temperature range was the performance of the long-term adaptability of nitrifying microorganisms. Meanwhile, several studies revealed that denitrification could be carried out in a wide temperature range (5～70 ℃), and it was positively related to temperature (Fan., 1995). However, the process will be inhibited when the temperature is too high or too low. The average ST in wet season was 27.4°C, conducive to the growth of denitrifying microorganisms, while that in dry season was 8.97°C, and the microbial activity was generally low (Sun et al., 2011). Furthermore, ST fluctuations were low both in wet season and dry season. Therefore, the effect of ST on N_2O emissions was masked by other factors, such as moisture content.

4.1.3 Effects of BIO and soil organic matter on GHG emissions

CO_2 and CH_4 emissions were higher in the riparian wetlands than in the grasslands, mainly because of greater vegetation cover. Typically, CO_2 emissions from riparian wetlands originate from plants and microorganisms, with plant respiration accounting for a large proportion in the growing season. Previous studies have shown that plant respiration accounts for 35–90% of the total respiration in the wetland ecosystem (Johnson-Randall and Foote, 2005). Good soil physicochemical properties and high soil total organic carbon (TOC) of riparian wetlands improve the activity of soil microorganisms and plant root respiration. Table 4 shows that BIO is significantly correlated with the CO_2 ($P < 0.05$) and CH_4 ($P < 0.01$) emissions. These results can be attributed to the significant linear positive correlation between the respiration rate and plant biomass (Lu et al., 2007). Higher plant biomass storage can achieve more carbon accumulation during photosynthesis and higher exudate release by the roots. This, in turn, promotes the

accumulation of soil organic matter. Increased amount of organic matter stimulates the growth and reproduction of soil microorganisms, ultimately promoting CO_2 and CH_4 emissions. Moreover, plants act as a gas channel for CH_4 transmission, and a larger amount of biomass promotes CH_4 emissions, given the increased number of channels. In transect T3, high CO_2 emissions observed at site L3 can be attributed to the relatively high levels of SMC, BIO, and soil nutrients, which stimulate the microbial respiration rates.

BIO had a weak correlation with N_2O emissions (Table 4), which indicates that plants increase N_2O production and emissions, although this may not be the most critical factor. Previous studies reported mechanisms where in the plants can absorb N_2O produced in the soil through the root system before releasing it into the atmosphere. Additionally, the root exudates of plants can enhance the activity of nitrifying and denitrifying bacteria in the soil, ultimately promoting the production of N_2O. Finally, oxygen stress caused by plant respiration can regulate the production and consumption of N_2O in the soil, eventually affecting the conversion of nitrogen in the soil (Koops et al., 1996; Azam et al., 2005).

Site L3 in transect T3 was covered by tall reeds, and its BIO was much higher than those of the other sites; thus, the data for this site were excluded from the correlation analysis.

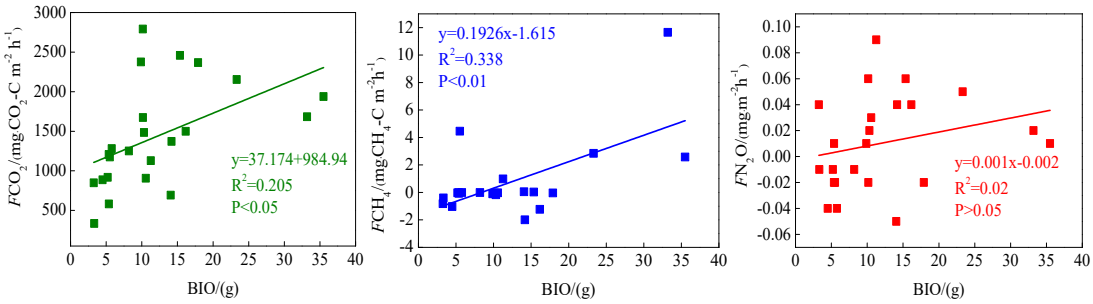

Fig. 7 Correlation between aboveground biomass (BIO) and GHG emissions (*F*)

Soil C:N ratio refers to the ratio of biodegradable carbonaceous organic matter and nitrogenous matter in the soil, and it forms the soil matrix with TOC. TOC decomposition provides energy for microbial activity, while the C:N ratio affects the decomposition of organic matter by soil microorganisms (Gholz et al., 2010). The correlation results (Fig. 8) indicate that TOC has a weak positive correlation with CO_2 emissions ($P > 0.05$), but soil C:N has a significant

447 negative correlation with CO_2 emissions ($P < 0.05$), indicating that nitrogen has a limiting effect
448 on soil respiration by affecting microbial metabolism. Liu et al. (2019) reported that N addition
449 promoted CO_2 emissions from wetlands soil, and the effect of organic N input was significantly
450 higher than those of inorganic N input. Organic carbon provides a carbon source for the growth of
451 plants and microorganisms, which boosts their respiration. Moreover, TOC has a significant
452 correlation with N_2O emissions ($P < 0.05$). Most heterotrophic microorganisms use soil organic
453 matter as carbon and electron donors (Morley N and Baggs E M., 2010). Soil carbon source has an
454 important influence on microbial activity. Nitrifying or denitrifying microorganisms need organic
455 matter to provide carbon source during the assimilation of NH_3 or NO_3^-. The high content of
456 organic matter in the soil can promote the abundance of heterotrophic nitrifying bacteria increases,
457 consume dissolved oxygen in the medium, and cause the soil to become more anaerobic, slowing
458 down autotrophic growth nitrifying bacteria. This reduces the nitrification rate, ultimately
459 promoting N_2O release. Enwall et al. (2005) studied the effect of long-term fertilization on soil
460 denitrification microbial action intensity. They found that the soil with long-term organic fertilizer
461 application has a significant increase in organic matter content, and consequently, a significant
462 increase in denitrification activity. Typically, low soil C:N ratios are favorable for the
463 decomposition of microorganisms, the most suitable range being between 10 and 12 (Pierzynski et
464 al., 1994). Table 4 shows that N_2O emissions are significantly related to the soil C:N ratios ($P <$
465 0.05), which means that denitrifying bacteria will use their endogenous carbon source for
466 denitrification when the external carbon source is insufficient. Moreover, incomplete
467 denitrification leads to the accumulation of NO_2-N, which is conducive to the N_2O release.
468 Meanwhile, due to the weak competitive ability of Nos to electrons, low C:N inhibits the synthesis
469 of Nos, which is also a reason for N_2O release. In this study, all the sites in transects T1–T4
470 exhibited similar soil C:N ratios in the optimum range (Table 1), which is favorable for microbial
471 decomposition. However, the soil C:N ratios in transect T5 were higher than those in the other
472 transects, especially in the dry lake bed. Therefore, transect T5 showed severe mineralization and
473 a low microbial decomposition rate.
474

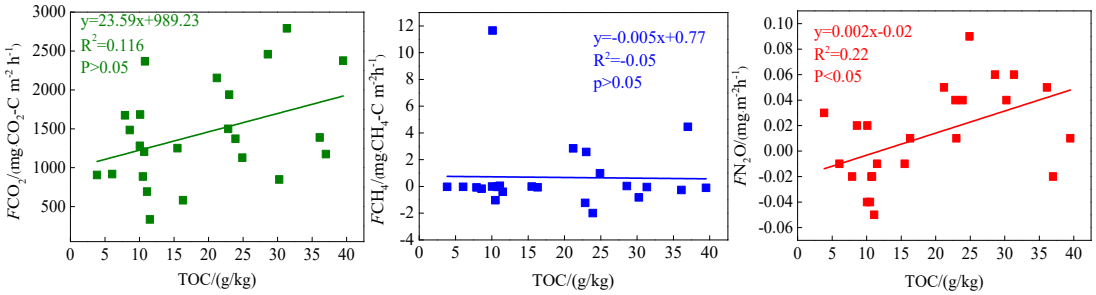

Fig. 8 Correlations between soil organic carbon (TOC) and GHG emissions (*F*)

Table 4. Correlations between CO_2, CH_4, and N_2O emissions and impact factors (n = 62)

GHG flux	ST10	ST20	SMC10	SMC20	TOC	ρ_b	C:N	pH	EC	BIO
CO_2	0.634**	0.592**	0.307*	0.216	0.393	−0.463**	−0.289*	−0.350**	−0.251*	0.491*
CH_4	−0.029	−0.051	0.346**	0.353**	−0.02	−0.129	−0.156	−0.127	−0.107	0.607**
N_2O	0.127	0.118	0.304*	0.356**	0.493*	−0.194	0.311*	0.137	0.504**	0.251

Note: 1. The analysis method used in the table is Pearson correlation analysis, and the numbers represent Pearson correlation coefficients.

2. * and ** denote significant and highly significant correlations ($P < 0.01$ and $P < 0.05$), respectively.

3. ST - soil temperature, SMC - soil moisture content, ρ_b - soil bulk density, soil C:N - soil carbon-nitrogen ratio, pH - soil pH, EC - soil electrical conductivity, BIO - aboveground biomass

4.2 Riparian wetlands as hotspots of GHG emissions

The results of this study emphasized that CO_2 emissions in the riparian wetlands were higher than those in the hillslope grasslands owing to a variety of factors. ST is an important factor affecting GHG emissions. Mclain and Martens (2006) showed that seasonal fluctuations in ST and SMC in semi-arid regions have important effects on CO_2, CH_4, and N_2O emissions in riparian soils. Poblador et al. (2017) studied the GHG emissions in forest riparian zones and suggested that the difference in the CO_2 and N_2O emissions in these zones is affected by the spatial gradient of the regional SMC. In this study, the upstream riparian wetlands are characterized by higher TOC, lower soil C:N ratio, and abundant BIO than the hillslope grasslands (Table 1). These soil conditions benefited the soil microbial activity, ultimately enhancing respiration as well as CO_2 emissions. However, CO_2 emissions in downstream areas were nearly identical to those in the grasslands because the wetlands gradually evolved into grasslands after their degradation. The

N_2O emissions showed spatial patterns similar to those of the CO_2 emissions because the CO_2 concentrations were closely related to nitrification and denitrification processes. High CO_2 concentrations can promote the carbon and nitrogen cycles in soil (Azam et al., 2005), increasing below ground C allocation associated with increased root biomass, root turnover, and root exudation in elevated pCO_2 plants provided the energy for denitrification in the presence of high available N, or that there was increased O_2 consumption under elevated pCO_2 (Baggs et al., 2003). Moreover, soil respiration increases during soil denitrification (Liu et al., 2010; Christensen et al., 1990). In this study, a weak correlation was observed between the CO_2 and CH_4 emissions in the riparian zones (r = 0.228), but CO_2 emissions were significantly correlated with N_2O emissions (r = 0.322, $P < 0.05$). The soil became anaerobic in the riparian areas as the SMC increased, and this was conducive to the survival of CH_4-producing bacteria and denitrification reactions, eventually leading to an increase in CH_4 and N_2O emissions. Jacinthe et al. (2015) reported that inundated grassland-dominated riparian wetlands were CH_4 sinks (-1.08 ± 0.22 kg·CH_4-C $ha^{-1}·yr^{-1}$), and Lu et al. (2015) also indicated that grasslands were CH_4 sinks. In our study, a marked water gradient across the transects led to the transformation of the soil from anaerobic to aerobic soil, which changed the wetland function as a CH_4 source or sink. Therefore, during the transition from the riparian wetlands to the hillslope grasslands, CH_4 emissions only appeared as sources in the near-stream sites and sinks at other sites.

Further, we compared the GHG emissions of riparian wetlands and hillslope grasslands around the Xilin River Basin with various types of grasslands (meadow grassland, typical grassland, and desert grassland) in the Xinlingol League in Inner Mongolia (Table 5). The CO_2 emissions in wet season decreased in the following order: upstream riparian wetlands > downstream riparian wetlands > hillslope grasslands > meadow grassland > typical grassland > desert grassland. Moreover, the upper riparian wetlands acted as source of CH_4 emissions, while the downstream transects and grasslands served as CH_4 sinks. Similarly, except for the downstream transects, N_2O emissions occurred as weak sources in different types of grasslands and upstream riparian wetlands. The GHG emissions showed similar spatial patterns in October. Although these estimates were made only in the growing season in August and the non-growing season in October, our results suggest that riparian wetlands are the potential hotspots of GHG emissions. Thus, it is important to study GHG emissions to obtain a comprehensive picture of the

role of riparian wetlands in climate change.

Table 5. GHG emission fluxes of riparian wetlands and grasslands

Sample plot		GHG emissions in August ($mg \cdot m^{-2} \cdot h^{-1}$)			GHG emissions in October ($mg \cdot m^{-2} \cdot h^{-1}$)			Reference
		CO_2	CH_4	N_2O	CO_2	CH_4	N_2O	
Wetlands of upstream transects (T1, T2, and T3)	n=13	1606.28 ± 697.78	1.417 ± 3.41	0.031 ± 0.03	182.35 ± 88.26	0.272 ± 0.49	0.002 ± 0.005	This study
Wetlands of downstream transects (T4 and T5)	n=7	1144.15 ± 666.50	−0.215 ± 0.45	−0.037 ± 0.05	98.13 ± 15.11	−0.015 ± 0.05	0.001 ± 0.01	
Hillslope grasslands of all transects	n=7	1071.54 ± 225.39	−0.300 ± 0.40	0.003 ± 0.03	77.68 ± 25.32	−0.048 ± 0.03	−0.002 ± 0.005	
Meadow grassland		166.39 ± 45.89	−0.038 ± 0.009	0.002 ± 0.001	-	-	-	Guo et al., 2017
Typical grassland		240.32 ± 87.56	−0.042 ± 0.025	0.037 ± 0.034	-	-	-	
Desert grassland		107.59 ± 54.10	−0.036 ± 0.015	0.003 ± 0.001	-	-	-	
Typical grassland		520.25 ± 59.07	−0.102 ± 0.012	0.007 ± 0.001	88.34 ± 9.84	−0.099 ± 0.003	0.005 ± 0.001	Zhang, 2019
Typical grassland		232.42 ± 18.90	−0.090 ± 0.005	0.004 ± 0.001	-	-	-	Chao, 2019
Typical grassland		265.23 ± 31.43	−0.185 ± 0.018	0.005 ± 0.001	189.41 ± 28.96	−0.092 ± 0.012	0.004 ± 0.001	
Meadow grassland		553.85	−0.163	0.003	47.73	−0.019	0.011	Geng, 2004
Typical grassland		308.60	−0.105	0.002	70.25	−0.029	0.007	

We roughly estimated the annual cumulative emissions of CO_2, CH_4, and N_2O from riparian wetlands and hillslope grasslands around the Xilin River Basin, and further calculated its global warming potential. Table 6 indicated that annual cumulative emissions of CO_2 and CH_4 decreased in the following order: upstream riparian wetlands > downstream riparian wetlands > hillslope grasslands, and N_2O in the following order: upstream riparian wetlands > hillslope grasslands > downstream riparian wetlands. In this study, we used the static dark-box method to measure CO_2

emissions, which does not consider the absorption and fixation of CO_2 by plants' photosynthesis. Therefore, the total annual cumulative CO_2 emissions are high. This result clearly showed that the significant impact of CO_2 emissions than CH_4 and N_2O emissions on global warming. The GWP depends on the cumulative emissions of the GHGs. GWP is shown as (Table 6): upstream riparian wetlands (13474.91 kg/hm^2) > downstream riparian wetlands (8974.12 kg/hm^2) > hillslope grasslands (8351.24 kg/hm^2). Therefore, both riparian wetlands and grasslands are the "sources" of GHGs on a 100-year time scale. The source strength of wetlands is higher than grasslands, further indicating that riparian wetlands are the hotspots of GHG emissions.

Table 6 Cumulative annual emission flux and global warming potential of GHGs in riparian wetlands and grasslands

Sample plot	CO_2/kg/hm^2	CH_4/kg/hm^2	N_2O/kg/hm^2	GWP/CO_2 kg hm^2
Wetlands of upstream transects (T1, T2, and T3)	13092.8±5378.16	12.36±26.40	0.25±0.23	13474.91±5828.68
Wetlands of downstream transects (T4 and T5)	9093.47±4831.82	-1.68±3.23	-0.26±0.40	8974.12±4912.75
Hillslope grasslands of all transects	8412.26±1614.26	-2.55±3.12	0.01±0.20	8351.24±1648.22

4.3 Effects of riparian wetland degradation on GHG emissions

The hydrology and soil properties showed evident differences among the transects because the downstream zone was dry all year due to the presence of the Xilinhot Dam (Fig. 1). The dam caused the degradation of the riparian wetlands, resulting in reduced GHG emissions. The average CO_2 emissions amounted to 1663 mg·m^{-2}·h^{-1} in the riparian wetlands in the upstream transects (T1, T2, and T3), while the downstream transects (T4 and T5) recorded an average of 1084 mg·m^{-2}·h^{-1}, 35% lower than the value in the upstream transects. The N_2O emissions from the riparian wetlands were lower in the downstream transects.

The wetland degradation first resulted in the continuous reduction of SMC, which led to the deepening of the wetland's aerobic layer thickness. Besides, SMC could affect ST's change and thus transformed CH_4 emissions from a source to a sink by affecting methanogens' activity (Yan et al., 2018). Secondly, the reduction of SMC impeded aboveground plants' physiological activities

and inhabited related enzymes' activities in the respiration process. Meanwhile, various enzyme reactions of underground microorganisms under water stress influence and reduced CO_2 emissions (Zhang et al., 2017). Finally, after wetland degradation, long-term drought caused too low SMC, which was not conducive to the growth of nitrifying and denitrifying bacteria, which caused the transformation of N_2O emissions from source to sink (Zhu et al., 2013). Table 1 shows that soil TOC in the upstream transects (average: 25.1 $g \cdot kg^{-1}$) is higher than that in the downstream transects (average: 8.41 $g \cdot kg^{-1}$). The relatively low SMC and the aerobic environment were conducive to the mineralization and decomposition of TOC. The degradation of plants in the wetlands led to the gradual reduction of BIO. Ultimately, the plant carbon source input of the degraded wetlands decreased, and the bare land temperature increased due to the reduced plant shelter. This accelerated the decomposition of TOC, leading to its decrease. This result indicates that wetland degradation caused the soil carbon pool's loss and weakened the wetland carbon source/sink function. These results are in agreement with those of Xia (2017).

The degraded wetlands also caused soil desertification and salinization, leading to a decline in the physical protection afforded by organic carbon and a reduction in soil aggregates. Thus, the preservation provided by organic carbon declined. TOC and SMC in the dry lake bed in transect T5 were relatively high, but GHG emissions were very low along this transect because soil pH values increased after the degradation of the lake soil, exceeding the optimum range required for microorganism activity. The soil C:N ratio was very high, resulting in severe mineralization and a low microbial decomposition rate, hence affecting the GHG emissions.

5. Conclusions

The riparian wetlands in the Xilin River Basin constitute a dynamic ecosystem. The present spatial and temporal transfers in the studied biogeochemical processes were attributed to the changes in SMC, ST, and soil substrate availability. Our simultaneous analysis of CO_2, CH_4, and N_2O emissions from riparian wetlands and hillslope grasslands in the Xilin River Basin revealed that the majority of the GHG emissions occurred in the form of CO_2. Moreover, our results clearly illustrated a marked seasonality and spatial pattern of GHG emissions along the transects and in the longitudinal direction (i.e., upstream and downstream). SMC and ST were two critical factors

589 controlling the GHG emissions. Moreover, abundant BIO promoted the CO_2, CH_4, and N_2O
590 emissions.

591 The riparian wetlands were the potential hotspots of GHG emissions in the Inner Mongolian
592 region. However, the degradation of wetlands transformed the area from a source to a sink for CH_4
593 and N_2O emissions, and reduced CO_2 emissions, which severely affected the wetland carbon cycle
594 processes. Our results show that the riparian wetlands have high CO_2 emissions, but wetlands are
595 CO_2 sink in the overall CO_2 balance general due to the photosynthesis of plants. Overall, our study
596 suggests that anthropogenic activities have significantly changed the hydrological characteristics
597 of the studied area, and will accelerate carbon loss from the riparian wetlands and further
598 influence the GHG emissions in the future.

599 ## Author Contributions

600 Xinyu Liu, Xixi Lu and Ruihong Yu designed the research framework and wrote the
601 manuscript. Xixi Lu and Ruihong Yu supervised the study. Xinyu Liu, Hao Xue, Zhen Qi,
602 Zhengxu Cao and Zhuangzhuang Zhang carried out the field experiments and laboratory
603 experiments analyses. Z.Z. drew GIS mapping in this paper. Tingxi Liu proofread the manuscript.
604 Heyang Sun contributed much in the revised version of our manuscript.

605 ## Acknowledgements

606 This study was funded by the National Key Research and Development Program of China
607 (grant no. 2016YFC0500508), Major Science and Technology Projects of Inner Mongolia
608 Autonomous Region (grant nos. 2020ZD0009 and ZDZX2018054), National Natural Science
609 Foundation of China (grant no. 51869014), Key Scientific and Technological Project of Inner
610 Mongolia (grant no. 2019GG019), and Open Project Program of the Ministry of Education Key
611 Laboratory of Ecology and Resources Use of the Mongolian Plateau (grant no. KF2020006).

612 ## Competing interests

613 The authors declare no conflicts of interest.

614 ## References

615 Azam F., Gill S., Farooq S.: Availability of CO_2 as a factor affecting the rate of nitrification in soil,
616 Soil Biology & Biochemistry, 37, 2141–2144, doi 10.1016/j.soilbio.2005.02.036, 2005.
617 Baggs E.M., Richter M., Cadisch G., Hartwig U.A.: Denitrification in grass swards is increased
618 under elevated atmospheric CO_2, Soil Biology and Biochemistry, 35, 729–732, doi

10.1016/S0038-0717(03)00083-X, 2003.

Beger M., Grantham H.S., Pressey R.L., Wilson K.A., Peterson E.L., Dorfman D., Lourival R., Brumbaugh D.R., Possingham H.P.: Conservation planning for connectivity across marine, freshwater, and terrestrial realms, Biological Conservation, 143, 565–575, doi 10.1016/j.biocon.2009.11.006, 2010.

Brady N C.: Nature and properties of soils, NewJersey: Prenflee-Hall. Inc., doi 10.2307/3894608, 1999.

Cao M., Yu G., Liu J., Li K.; Multi-scale observation and cross-scale mechanistic modelling on terrestrial ecosystem carbon cycle, Science in China Ser. D Earth Sciences, 48, 17–32, doi 10.1360/05zd0002, 2005.

Chao R.: Effects of Simulated Climate Change on Greenhouse Gas Fluxes in Typical Steppe Ecosystem, Inner Mongolia University, 2019.

Cheng S and Huang J.: Enhanced soil moisture drying in transitional regions under a warming climate, Journal of Geophysical Research-Atmospheres, 121, 2542–2555, doi 10.1002/2015JD024559, 2016.

Christensen S., Simkins S., Tiedje J M.: Temporal Patterns of Soil Denitrification: Their Stability and Causes, Soil Science Society of America Journal, 54, 1614, doi 10.2136/sssaj1990.03615995005400060017x, 1990.

Ding W., Cai Z., Tsuruta H.: Cultivation, nitrogen fertilization, and set‐aside effects on methane uptake in a drained marsh soil in Northeast China, Global Change Biology, 10, 1801‐1809, doi 10.1111/j.1365-2486.2004.00843.x, 2010.

Enwall K., Philippot L., Hallin S.: Activity and composition of the denitrifying bacterial community respond differently to long-term fertilization, Applied and Environmental Microbiology, 71, 8335-8343, doi 10.1128/AEM.71.12.8335-8343.2005, 2005.

Fan X.: Research on nitrification potential and denitrification potential of soil in several farmland in China, Nanjing Institute of Soil Sciences, Chinese Academy of Sciences, 1995.

Ferrón S., Ortega T., Gómez-Parra A., Forja J.M.: Seasonal study of dissolved CH_4, CO_2 and N_2O in a shallow tidal system of the bay of Cádiz (SW Spain), Journal of Marine Systems, 66, 244–257, doi 10.1016/j.jmarsys.2006.03.021, 2007.

Geng H.: Study on Charactors of CO_2, CH_4, N_2O Fluxes and the Relationship between Them and

649 Environmental Factors in the Temperate Typical Grassland Ecosystem, Northwest Agriculture &
650 Forestry University, 2004.
651 Gholz H.L., Wedin D.A., Smitherman S.M., Harmon M.E., Parton W.J.: Long-term dynamics of
652 pine and hardwood litter in contrasting environments: toward a global model of decomposition,
653 Global Change Biology, 6, 751–765, doi 10.1046/j.1365-2486.2000.00349.x, 2000.
654 Gou Q., Qu J., Wang G., Xiao J., Pang Y.: Progress of wetland researches in arid and
655 semi-ariregions in China, Arid Zone Research, 1001–4675, 213–220, 2015.
656 Guo X., Zhou D., Li Y.: Net Greenhouse Gas Emission and Its Influencing Factors in Inner
657 Mongolia Grassland, Chinese Grassland Society, 2017.
658 Heilman J.L., Cobos D.R., Heinsch F.A., Campbell C.S., McInnes K.J.: Tower-based conditional
659 sampling for measuring ecosystem-scale carbon dioxide exchange in coastal wetlands, Estuaries,
660 22, 584–591, doi 10.2307/1353046, 1999.
661 Inubushi K., Furukawa Y., Hadi A., Purnomo E., Tsuruta H.: Seasonal changes of CO_2, CH_4 and
662 N_2O fluxes in relation to land-use change in tropical peatlands located in coastal area of South
663 Kalimantan, Chemosphere, 52, 603–608, doi 10.1016/s0045-6535(03)00242-x, 2003.
664 IPCC.: Climate Change 2013: The Physical Science Basis. Contribution of Working, Working
665 Group I of the IPCC, 43, 866–871, 2013.
666 Jacinthe P.A., Vidon P., Fisher K., Liu X., Baker M.E.: Soil Methane and Carbon Dioxide Fluxes
667 from Cropland and Riparian Buffers in Different Hydrogeomorphic Settings, Journal of
668 Environment Quality, 44, 1080–1115, doi 10.2134/jeq2015.01.0014, 2015.
669 Johnson-Randall L.A., Foote A.L.: Effects of managed impoundments and herbivory on wetland
670 plant production and stand structure, Wetlands, 25, 38–50, doi
671 10.1672/0277-5212(2005)025[0038:eomiah]2.0.co;2, 2005.
672 Koops J.G., Oenema O., Beusichem M.L.: Denitrification in the top and sub soil of grassland on
673 peat soils, Plant and Soil, 184, 1–10, doi 10.1007/bf00029269, 1996.
674 Kou X.: Study on Soil Physicochemical Properties and Bacterial Community Characteristics of
675 River Riparian Wetland in Inner Mongolia Grassland, Inner Mongolia University, 2018.
676 Liu C.: Effects of Nitrogen Addition on the CO_2 Emissions in the Reed (Phragmites australis)
677 Wetland of the Yellow River Delta, China, Liaocheng University, 2019.
678 Liu C., Xie G., Huang H.: Shrinking and drying up of Baiyangdian Lake wetland: a natural or

679 human cause? Chinese Geographical Science, 16, 314–319, 2006.
680 Liu F., Liu C., Wang S., Zhu Z.: Correlations among CO_2, CH_4, and N_2O concentrations in soil
681 profiles in central Guizhou Karst area, Chinese Journal of Ecology, 29, 717–723, doi
682 10.1016/S1872-5813(11)60001-7, 2010.
683 Liu J., Wang J., Li Z., Yu J., Zhang X., Wang C., Wang Y.: N_2O Concentration and Its Emission
684 Characteristics in Sanjiang Plain Wetland, Chinese Journal of Environmental Science, 24, 33–39,
685 2003.
686 Lu Y., Song C., Wang Y., Zhao Z.: Influence of plants on CO_2 and CH_4 emission in wetland
687 ecosystem, Acta Botanica Boreali-Occidentalia Sinica, 27, 2306–2313, 2007.
688 Lu Z., Du R., Du P., Li Z., Liang Z., Wang Y., Qin S., Zhong L.: Effect of mowing on N_2O and
689 CH_4 fluxes emissions from the meadow-steppe grasslands of Inner Mongolia, Frontiers of Earth
690 Science, 9, 473–486, doi 10.1007/s11707-014-0486-z, 2015.
691 Lv M., Sheng L., Zhang L.: A review on carbon fluxes for typical wetlands in different climates of
692 China, Wetland Science, 11, 114–120, doi CNKI:SUN:KXSD.0.2013-01-020, 2013.
693 Malhl S.S., Mcgill W.B.: Nitrification in three Alberta soils: effects of temperature, moisure and
694 substrates concentration, Soil Biology and Biochemistry, 14, 393–399, doi
695 10.1016/0038-0717(82)90011-6 1982.
696 Mclain J E T., Martens D.A.: Moisture controls on trace gas fluxes in semiarid riparian soils, Soil
697 Science Society of America Journal, 70, 367, doi 10.2136/sssaj2005.0105, 2006.
698 Meng W., Wu D., Wang Z.: Control factors and critical conditions between carbon sinking and
699 sourcing of wetland ecosystem, Ecology and Environmental Sciences, 20, 1359–1366, doi
700 10.1016/S1671-2927(11)60313-1, 2011.
701 Mitsch W.J., Gosselink J.G.: Wetlands (Fourth Edition), John Wiley & Sons Inc.: Hoboken, New
702 Jersey, USA, 2007.
703 Mitsch W.J., Gosselink J.G., Anderson C.J., Anderson, C. J.: Wetland ecosystems: John Wiley &
704 Sons, 2009.
705 Moldrup P., Olesen T., Schjønning P., Yamaguchi T., Rolston D.E.: Predicting the gas diffusion
706 coefficient in undisturbed soil from soil water characteristics, Soil Science Society of America
707 Journal, 64, 1588–1594, doi 10.2136/sssaj2000.64194x, 2000.
708 Morley N., Baggs E.M.: Carbon and oxygen controls on N_2O and N_2 production during nitrate

reduction, Soil Biology＆Biochemistry, 42, 1864-1871, doi 10.1016/j.soilbio.2010.07.008, 2010.

Naiman R.J., Decamps H.: The ecology of interfaces: Riparian zones, Annual Review of Ecology & Systematics, 28, 621–658, doi 10.2307/2952507, 1997.

National Agricultural Technology Extension Service Center (NATESC).: Technical specification for soil analysis, 2006.

Niu C., Wang S., Guo Y., Liu W., Zhang J.: Studies on variation characteristics of soil nitrogen forms, nitrous oxide emission and nitrogen storage of the Phragmites australis-dominated land/inland water ecotones in Baiyangdian wetland, Journal of Agricultural University of Hebei, 40, 72–79, 2017.

Pierzynski G M S., J.T.,Vance, G.F.: Soils and Environmental Quality, 1994.

Poblador S., Lupon A., Sabaté S., Sabater F.: Soil water content drives spatiotemporal patterns of CO_2 and N_2O emissions from a Mediterranean riparian forest soil, Biogeosciences Discussions, 14, 1–28, doi 10.5194/bg-14-4195-2017, 2017.

Qin S., Tang J., Pu J., Xu Y., Dong P., Jiao L., Guo J.: Fluxes and influencing factors of CO_2 and CH_4 in Hangzhou Xixi Wetland，China, Earth and Environment, 44, 513–519, 2016.

Sjögersten S., Wal R V.D., Woodin S.J.: Small-scale hydrological variation determines landscape CO_2 fluxes in the high Arctic, Biogeochemistry, 80, 205–216, doi 10.2307/20456398, 2006.

Sun Y., Wu H., Wang Y.: The influence factors on N_2O emissions from nirification and denitrification reaction, Ecology and Environmental Sciences, 20, 384–388, doi 10.1631/jzus.B1000275, 2011.

Tong C., Wu J., Yong S., Yang J., Yong W.: A landscape-scale assessment of steppe degradation in the Xilin River Basin, Inner Mongolia, China, Journal of Arid Environments, 59, 133–149, doi 10.1016/j.jaridenv.2004.01.004, 2004.

Ulrike R., Jürgen A., Rolf R., Wolfgang M.: Nitrate removal from drained and reflooded fen soils affected by soil N transformation processes and plant uptake, Soil Biology and Biochemistry, 36, 77-90, doi 10.1016/j.soilbio.2003.08.021, 2004.

Waddington J.M., Roulet N.T.: Carbon balance of a boreal patterned peatland, Global Change Biology, 6, 87–97, doi 10.1046/j.1365-2486.2000.00283.x, 2000.

Whiting G.J., Chanton J.P.: Greenhouse earbon balance of wetlands: methane emission versus carbon sequestration, Tellus B, 53, 521-528, doi 10.3402/tellusb.v53i5.16628, 2001.

WMO.: WMO Statement on the State of the Global Climate in 2017, World Meteorological Organization, 2018.

Xi X., Zhu Z., Hao X.: Spatial variability of soil organic carbon in Xilin River Basin, Research of Soil and Water Conservation, 24, 97–104, 2017.

Xia P., Yu L., Kou Y., Deng H., Liu J.: Distribution characteristics of soil organic carbon and its relationship with enzyme activity in the Caohai wetland of the Guizhou Plateau, Acta Scientiae Circumstantial, 37, 1479–1485, doi 10.13671/j.hjkxxb.2016.0129, 2017.

Xu H., Cai Z., Yagi K.: Methane Production Potentials of Rice Paddy Soils and Its Affecting Factors, Acta Pedologica Sinica, 45, 98–104, doi 10.1163/156939308783122788, 2008.

Yan L., Zhang X., Wang J., Li Y., Wu H., Kang X.; Drainage effects on carbon flux and carbon storage in swamps, marshes, and peatlands, Chin J Appl Environ Biol, 24, 1023–1031, doi 10.19675/j.cnki.1006-687x.2017.11031, 2018.

Yu P., Zhang J., Lin C.: Progress of influence factors on N_2O emission in farmland soil, Environment and sustainable development, 20–22, 2006.

Zhang D.: Effects of Different Grazing Intensities on Greenhouse Gases Flux in Typical Steppe of Inner Mongolia, Inner Mongolia University, 2019.

Zhang Y., Hao Y., Cui L., Li W., Zhang X., Zhang M., Li L., Yang S., Kang X.: Effects of extreme drought on CO_2 fluxes of Zoige alpine peatland, Journal of University of Chinese Academy of Sciences, 34, 462-470, 2017.

Zhang Z., Hua L., Yin X., Hua L., Gao J.: Nitrous oxide emission from agricultural soil land some influence factors, Journal of Capital Normal University: Natural Science Edition, 26, 114–120, 2005.

Zhu X., Song C., Guo Y., Shi F., Wang L.: N_2O emissions and its controlling factors from the peatlands in the Sanjiang Plain, China Environmental Sciences, 33, 2228 – 2234, 2013.

Zona D., Oechel W.C., Kochendorfer J., Paw U K.T., Salyuk A.N., Olivas P.C., Oberbauer S.F., Lipson D.A.: Methane fluxes during the initiation of a large-scale water table manipulation experiment in the Alaskan Arctic tundra, Global Biogeochem Cycles, 23, doi 10.1029/2009gb003487, 2009.